ELSEVIER

Contents lists available at ScienceDirect

Analytical Biochemistry

journal homepage: www.elsevier.com/locate/yabio





DNA-facilitated target search by nucleoproteins: Extension of a biosensor-surface plasmon resonance method

Tam D. Vo a, 1, Amelia L. Schneider Gregory M.K. Poon b, W. David Wilson b, a, b, a

- * Department of Chemistry, Georgia State University, USA
- b Center for Diagnostics and Therapeutics, Georgia State University, USA

ARTICLE INFO

Keywordx
Biosensor
Surface plasmon resonance
DNA-Facilitated dissociation
Intersegmental translocation
Protein/DNA interactions
BTS transcription Factors

ABSTRACT

To extend the value of biosensor-SPR in the characterization of DNA recognition by nucleoproteins, we report a comparative analysis of DNA-facilitated target search by two ETS-family transcription factors: Elk1 and ETV6. ETS domains represent an attractive system for developing biosensor-based techniques due to a broad range of physicochemical properties encoded within a highly conserved DNA-binding motif. Building on a biosensor approach in which the protein is quantitatively sequestered and presented to immobilized cognate DNA as nonspecific complexes, we assessed the impact of intrinsic cognate and nonspecific affinities on long-range (intersegmental) target search. The equilibrium constants of DNA-facilitated binding were sensitive to the intrinsic binding properties of the proteins such that their relative specificity for cognate DNA were reinforced when binding occurred by transfer vs. without nonspecific DNA. Direct measurement of association and dissociation kinetics revealed ionic features of the activated complex that evidenced DNA-facilitated dissociation, even though Elk1 and ETV6 harbor only a single DNA-binding surface. At salt concentrations that masked the effects of nonspecific pre-binding at equilibrium, the dissociation kinetics of cognate binding were nevertheless distinct from conditions under which nonspecific DNA was absent. These results further strengthen the significance of long-range DNA-facilitated translocation in the physiologic environment.

1. Introduction

The localization of sequence-specific nucleoproteins, and presumably other ligands as well, at their target site involves prior association and translocation along nonspecific DNA [1,2]. These transient dynamics may be short-range sliding or hopping over short contiguous stretches, or long-range translocation between segments that are distant (up to over many kbp) in sequence. The biological significance of long-range transfer is increasing due to recent attention on genomic organization in eukaryotes into large-scale units such as topologically associating domains, or TADs [3]. TADs bring into close spatial proximity up to hundreds of genes at the level of chromatin [4]. Functionally similar, albeit less complex long-range topologies are also characteristic in prokaryotes such as bacteria [5]. There is therefore a need for experimental methods that can directly measure the properties of long-range translocation of DNA-binding proteins to their target sites.

Since the classic studies on the kinetics of site binding by the lac repressor and cAMP receptor protein, many experimental techniques have been developed to probe the role of DNA-mediated diffusion in site localization by DNA-binding proteins. While particle-tracking techniques [e.g., 6, 7, 8] offer unique opportunities to directly observe and acquire statistics on the stochastic behavior of individual units, ensemble methods are highly complementary and retain significant value in terms of accessibility to the community. To this end, we recently introduced a biosensor-based, surface plasmon resonance (SPR)-detected approach for gaining insight into the DNA-facilitated target search by DNA-binding proteins [9]. This technique involves measuring the kinetics of association and dissociation to immobilized DNA by protein in the flow solution with and without an excess of nonspecific DNA. When controlled as a function of ionic conditions via the bulk salt concentration, this method provides additional quantitative information about the electrostatic contributions of target search.

Applying this technique to the DNA-binding domain of ETV6, an ETS-family transcription factor implicated in cancers of the prostate and blood, we previously measured DNA-facilitated target search by ETV6 [9]. DNA-binding proteins with multimeric structures allow them to

^{*} Corresponding authors. Department of Chemistry, Georgia State University, Atlanta, GA 30303, USA. E-mail addresses: gpoon@gsu.edu (G.M.K. Poon), wdw@gsu.edu (W.D. Wilson).

Current address: National Cancer Institute, National Institutes of Health, Bethesda, MD 20892, USA.

contact two or more DNA segments simultaneously and execute long-range intersegmental transfer via a monkey-bar mechanism [10 13]. However, the corresponding behavior for ETV6 and myriad other proteins with only single DNA-contact surfaces that bind DNA as monomers is not well understood. More generally, there is a lack of knowledge on intrinsic affinities for cognate and nonspecific DNA as parameters of whether long-range target search occurs and, if so, its effective properties in a mixed-DNA environment.

To make progress, we extended the SPR-based technique further to address several new questions about long-range DNA-facilitated translocation. 1) How do the intrinsic affinities for cognate and nonspecific DNA impact the characteristics of long-range translocation? 2) What is the propensity for long-range transfer by highly target-specific nucleoproteins such as many transcription factors? 3) What are the molecular signatures of DNA-facilitated dissociation, an emerging feature in our knowledge of DNA-facilitated dynamics, that are detectable by this technique? For these studies, ETS-family transcription factors are attractive models due to the broad range of biophysical characteristics that are encoded in a tightly conserved DNA-binding motif. This combination of physicochemical diversity and structural homology facilitates a comparative approach that has shown utility in other lines of inquiry [14 17]. To leverage the existing data for ETV6 [9], we carried out a comparative study with Elk1, an ETS member that binds with very high affinity to cognate motifs as reported by gel mobility shift [18]. We expect a quantitative comparison of the two structural homologs by biosensor-SPR to generate significant new insight into the features that impact cognate target binding by long-range target search.

2. Material and methods

Nucleic acids. DNA hairpins were purchased from Integrated DNA Technologies (Coralville, IA) and annealed to form duplex binding sites as previously described [16]. Salmon sperm DNA was purchased from Sigma-Aldrich (D1626) and used without further purification. The concentrations of DNA sequences (ETS consensus in bold) were determined by UV absorption at 260 nm using the following extinction coefficients at 260 nm: SC1 (5 -CGG CCA AGC CGG AAG TGA GTG CC-3): 366,479 M $^{-1}$ cm $^{-1}$, E74 (5 -CTG AAT AAC CGG AAG TAA CTC ATC-3): 500,700 M $^{-1}$ cm $^{-1}$, salmon sperm: 6600 (M bp) $^{-1}$ cm $^{-1}$. A full-length clone of human Elk1 (cDNA clone MGC:64973) open reading frame was purchased from the Harvard Plasmid Repository.

Molecular cloning. A construct encoding the minimal DNA-binding (ETS) domain of Elk1 (human residues 1 to 93, without any of the auto-inhibitory or other domains) was amplified from the full-length clone by PCR and ligated into the NcoI/XhoI sites of pET28b. The cloned construct consists of the open reading frame for ELK1 ETS domain plus additional sequences encoding a C-terminal thrombin cleavage site followed by a 6xHis tag. The recombinant plasmid was transformed into DH5 $E.\ coli$ and sequence-verified by Sanger sequencing.

Protein expression and purification. Heterologous expression of Elk1 in BL21*(DE3) *E. coli* was performed as previously described [15,19]. In brief, cells in log phase were induced for 4 h with 0.5 mM IPTG, harvested by centrifugation, lysed by sonication, and extracted by immobilized metal affinity chromatography on Co-NTA resin (Gold Biotechnology). After cleaving the C-terminal 6xHis tag with thrombin overnight at room temperature, the target protein was purified by cation exchange chromatography on Sepharose SP (GE). Protein concentrations were determined by UV absorption at 280 nm using an extinction coefficient of 25,440 M $^{-1}$ cm $^{-1}$.

Biosensor-surface plasmon resonance (SPR). SPR measurements were performed with a Biacore T200 biosensor (GE) in a 4-channel system as previously described [20,21]. In brief, 5 biotinylated DNA sequences of interest were immobilized on CM5 chips on flow cells 2 to 4 at low density to \sim 150 RU (response unit). Flow cell 1 was used as a reference cell and contained no immobilized DNA. The experimental buffer

contains 25 mM Na_2HPO_4/NaH_2PO_4 , pH 7.4, 1 mM EDTA, 0.05% v/v P20 surfactant and sufficient NaCl to achieve the desired total Na concentrations. Mass transfer was minimized by running the fluidics at a high flow rate of 50 L/min [Fig. 1]. Equilibrium dissociation constants (K_D) were estimated from the steady-state signal observed in the sensorgrams as follows:

where RU_{obs} is the change in response unit when a protein binds to DNA at equilibrium state, RU_{max} is the response at saturation, and C_f is the free protein concentration. Alternatively, K_D was computed from the apparent association and dissociation kinetic rate constants $(k_a$ and $k_d)$ fitted from the time-dependent data:

The detailed procedures for both approaches have been extensively described [20 22]. Salt dependence of $K_{\rm D}$ values is analyzed by linear regression on logarthmic scales. Data exhibiting chevrons is fitted with a piecewise function:

(3)

where m_1 and m_2 are the slopes of the two segments, b_1 is the intercept of the first segment on the ordinate, and x_c is the position of the chevron on the abscissa.

Bioinformatic motif analysis. DNA motifs for Elk1 and ETV6 were culled from the CIS-BP Database [23] as position-weighted matrices. Rendering of information content-weighted DNA logos was performed using enoLOGOS [24].

3. Results and discussion

Elk1 is a highly selective DNA-binding protein. Our first objective is to quantify the intrinsic specificity of DNA recognition by Elk1. Immobilized DNA harboring a cognate site (5 -GCCGGAAGTG-3) was exposed to flow solutions containing graded concentrations of purified ETS domain of Elk1 (without auto-inhibitory or any other domains that modify binding) [Fig. 2A]. The protein solution flowed at a high rate (50 L/min) to minimize mass transfer to and from the biosensor chip. To ensure that the SPR measurements reflected the intrinsic affinities characteristic of direct target search from free solution, the cognate DNA was immobilized as a short hairpin oligomer (24 bp) such that local translocation around the cognate site would be negligible. Across a range of salt concentrations up to 0.6 M in the flow solution, the steady state data was well described by fitting to a 1:1 model according to Eq. (1) [Fig. 2B]. The maximum SPR signal (in RU) also corresponded to the expected MW of a 1:1 Elk1/DNA complex. Finally, the time-dependent RU signal was independently fitted to a 1:1 model to extract firstorder kinetic rate constants. The ratios of these rate constants, following Eq. (2), yielded equilibrium constants that agreed with the steady-state values within experimental uncertainty [Table S1, Supporting Information]. The results therefore indicated that Elk1 bound SC1 with 1:1 stoichiometry across the full range of salt concentrations used.

The salt dependence of the equilibrium constants reports the release of counter-ions from the DNA upon binding. When monovalent ions are used (as the case here), which can be related to the number of DNA phosphate contacts via the polyelectrolyte theory as follows:

 $m_{\rm obs}$ is proportional to the number of DNA phosphate contacts |z| by a coefficient consisting of 0.88 for B-form DNA, which

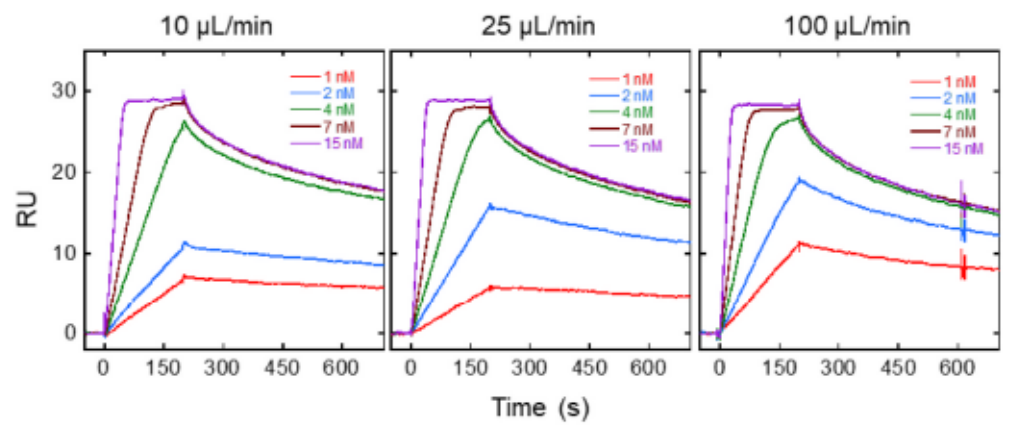


Fig. 1. Representative sensorgrams of Elk1 binding E74 at 0.15 M Na+ in the presence of 100 µM bp salmon sperm DNA with different flow rates. Sensorgrams record the SPR-detected time-dependent interactions on the biosensor exposed to ligands in the flow solution passing at 10, 25, or 100 μL/min. Protein was removed from the flow solution at 200 s, at which point dissociation ensues. The mass transfer effect was significant at 10 µL/min. Increasing the flow rate reduced the impact of the mass transfer. However, there was no significant further improvement between 25 and 100 µL/min. A flow rate of 50 µL/min was chosen for this study to avoid running out of flow solution at higher flow rates during the experiment.

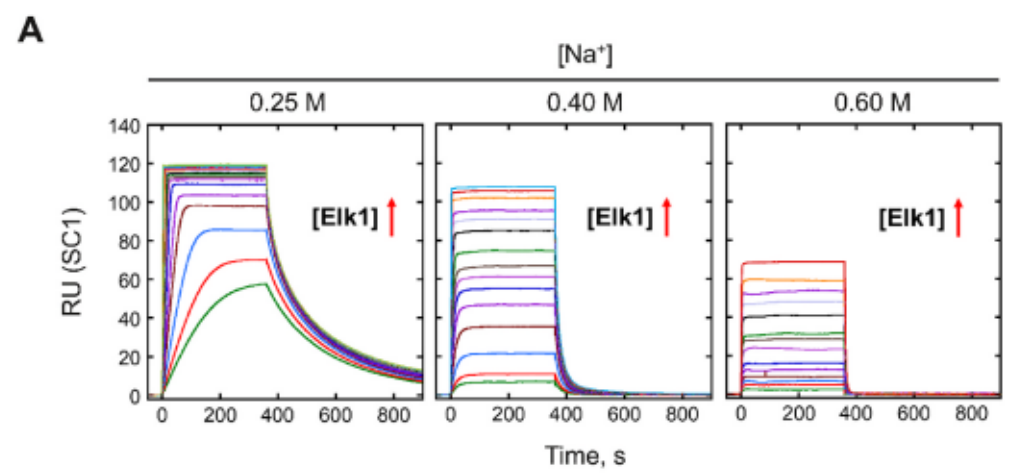
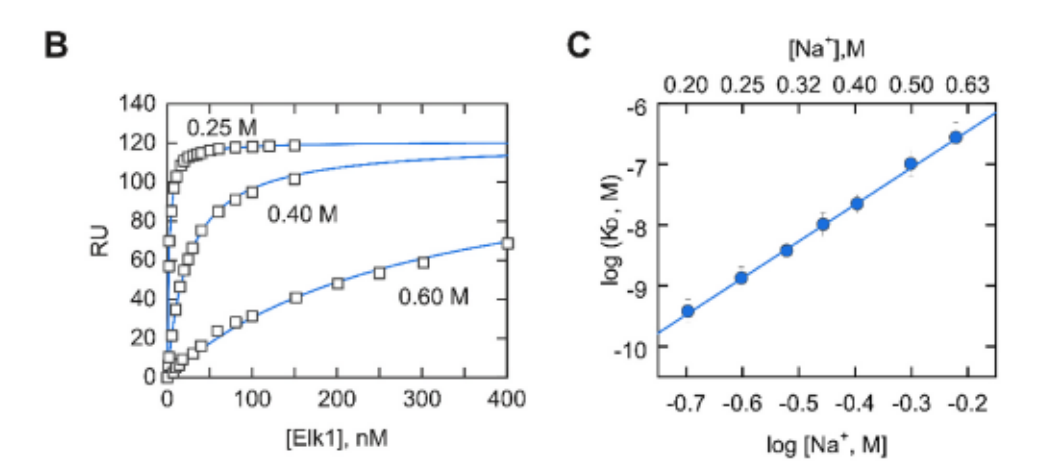


Fig. 2. Biosensor-SPR analysis of intersegmental target search by the DNAbinding domain of Elk1 to the SC1 site. A, Representative sensorgrams of DNA binding to the SC1 site by graded concentrations of RIk1 at the indicated bulk salt concentrations. Elk1 concentrations were varied from 1 to 150 nM at 0.2 M Na⁺, from 1 to 250 nM at 0.4 M Na+, and from 5 to 400 nM at 0.6 M Na+. B, Steady-state fits of the binding signal in the plateau region of the sensorgram with a 1:1 binding model at different salt concentrations. C, Salt dependence of the equilibrium dissociation constants of Elk1 with SC1. Error bars represent S.E. of the fits. The log-log salt-dependent slope is 6.0 ± 0.1 .



combines the effects of counterion condensation ($\Psi_{\rm C}=0.76$) and ion screening ($\Psi_{\rm S}=0.12$) [25]. A correction for end-effects is applied for oligomeric dsDNA harboring N_p phosphates [26]. For the 24-bp synthetic hairpins used in the SPR experiments, the corrected coefficient is $\phi=0.77$. Negative values of $\Delta m_{\rm obs}$ denote a release of counter-ions. Based on the measured salt-dependent binding [Fig. 2C], Elk1 contacted $|z|=7\pm1$ phosphates on the SC1 sequence, matching the number observed in the co-crystal cognate complex of Elk1 [27]. The data therefore confirmed biosensor-SPR as an accurate analytical technique for measuring cognate Elk1/DNA binding.

The stronger cognate binding by Elk1 suggests a potential for higher

sequence specificity than ETV6, a highly conserved structural homolog [Fig. 3A], provided that Elk1 binds nonspecific DNA with comparable or weaker affinity. When we attempted to measure Elk1 binding to an immobilized nonspecific sequence by SPR, the biosensor did not register significant signal even at the highest concentration of protein used (500 nM) in the flow solution [Fig. S1, Supporting Information]. The nonspecific affinity for Elk1 was too low for biosensor-SPR detection. We therefore used reported data on nonspecific binding by Elk1 to mixed-sequence salmon sperm DNA as measured by a fluorescence quench method [28]. The nonspecific measurements, which tracked the intrinsic tryptophan fluorescence of the proteins, were analyzed by the

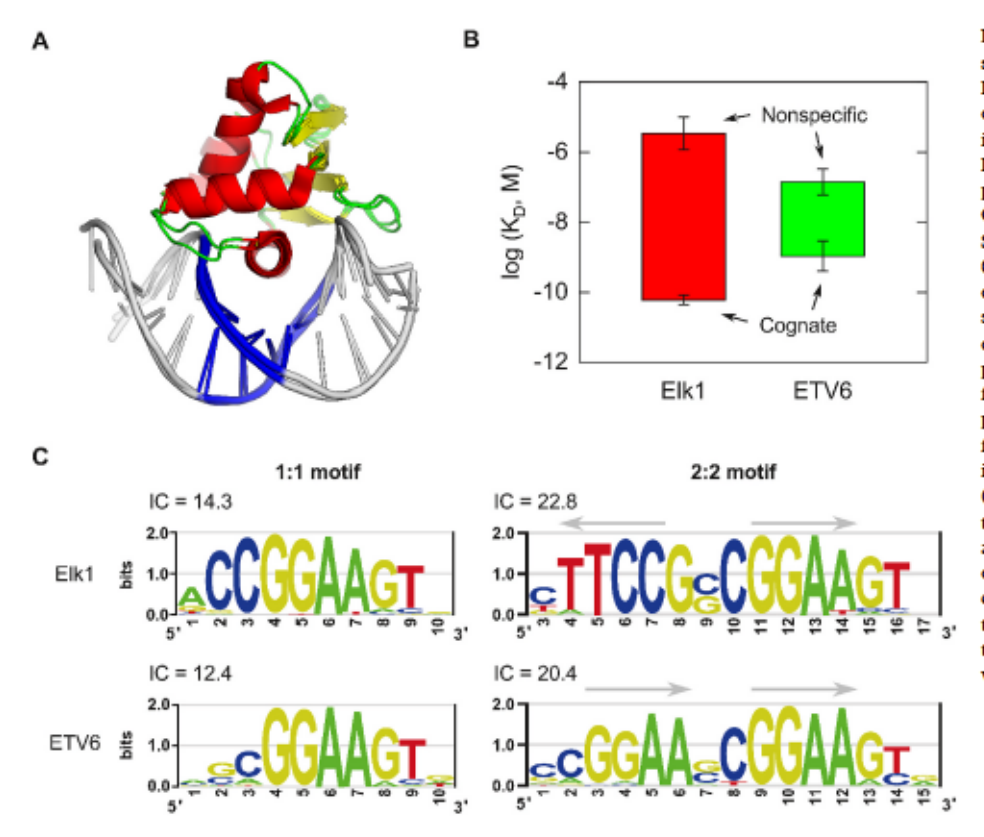


Fig. 3. Comparative target selectivity of two structurally conserved ETS domains: Elk1 and RTV6. A Structural alignment of the RTS domains of Elk1 (PDB: 1DUX) and ETV6 (4MHG) as observed in their co-crystallographic complexes with cognate DNA. The RMSD for the protein was 0.7 Å. The proteins are colored by secondary structure. The 5'-GGAA-3' core consensus is colored in blue. B, Summary of affinities for the two ETS homologs at 0.15 M Na+. Extrapolated equilibrium dissociation constants (±S.E.) from steady-state analysis are shown for cognate binding. Nonspecific dissociation constants (in M bp) from fluorescence quench experiments are taken from Fig. S2 for Elk1 and [9] for ETV6. C, DNA logos from published position-weighted matrices for genomic binding by full-length Elk1 and ETV6. Motifs with the highest information contents (IC) in the case of isolated (left) and tandem (right) site binding were shown, truncated, and shifted as appropriate for alignment and fair comparison. The maximum IC in binary bits of a motif of length N is 2 N. Arrows denote the direction of cognate sites in the 5'-GGAA-3' direction. (For interpretation of the references to color in this figure legend, the reader is referred to the Web version of this article.)

McGhee-von Hippel formalism [29] to yield intrinsic equilibrium dissociation constants [Fig. S2, Supporting Information]. Indeed, Blk1 exhibited weaker nonspecific binding compared with available data for BTV6 [9] under the same conditions. Combined with its strong cognate affinity, the data established Blk1 as a highly selective DNA-binding protein, exhibiting a specificity (cognate/nonspecific) ratio of >10⁵ [Fig. 3B]. In contrast, ETV6 exhibited a specificity ratio of 10².

To determine whether the selectivity differences in vitro reflect the behavior of native proteins in cells, we analyzed genomic binding by native Elk1 and ETV6 reported in published chromatinimmunoprecipitation sequencing (ChIP-Seq) studies [30]. The ensemble of sequences, as represented by DNA logos, provide a direct indicator of specificity in terms of the additive informational content (IC) at each position of the motif [24]. Expressed as binary bits, the IC of each position ranges from 0 (all four bases equally probable) to 2 (selection of a single nucleobase). Summation of the ICs over a site yields the IC for the whole binding motif. As shown in [Fig. 3C], Elk1 and ETV6 occupy genomic DNA as monomers in two distinct modes: bound to isolated single sites or to tandem cognate sequences. While the 1:1 complex is homologous for both proteins, consistent with their co-crystal structures, their 2:2 motifs run in different directions. The bases flanking one of the core consensus in the 2:2 Elk1-binding motif correspond to SC1. The two copies of core consensus (5'-GGAA-3') runs anti-parallel for Elk1 but are in parallel for ETV6, suggesting opposite orientations for the bound proteins. For the fairest comparison, we analyzed the longest DNA logos that span corresponding positions for both ETS members. The sequence-specific nature of both proteins is evident in the high IC at the core consensus, regardless of binding mode. However, selectivity at flanking positions is more variable, and quantitation of the overall IC shows higher values for Elk1 relative to ETV6. In 1:1 motifs, Elk1 exhibits 2 extra bits (10% over a 10-bp site) of IC over ETV6. This difference is preserved between their 2:2 complexes, suggesting that any protein-protein interaction between bound ETV6 at the tandem sequences does not overcome for the intrinsic deficit as a

monomer. Thus, agreement with genomic data suggests that the target selectivity determined biophysically reflects genomic occupancy in vivo.

Impact of sequence selectivity on target search. The substantially greater selectivity of Elk1 over ETV6, given in a highly homologous scaffold, suggested the two ETS relatives as an excellent pair for probing the impact of site selectivity in DNA-facilitated target search. To mimic long-range translocation, excess concentration of salmon sperm DNA (100 µM bp) was added to the flow solution to ensure that Elk1 was quantitatively trapped in a nonspecific complex at low salt. To minimize mass transfer, the flow solution was kept at a high flow rate of 50 µL/min (Fig. 1). Under these conditions, unbound protein was no longer a significantly populated state at equilibrium, and SPR-detected binding represented the effective transfer of nonspecifically (ns) bound Elk1 from the flow solution to its specific (sp) target sequence in the immobilized oligomer:

We define the coefficient Δm_{tr}

$$\Delta m_{\rm lr} = \Delta m_{\rm sp} - \Delta m_{\rm ns} \tag{6}$$

as the change in ion number for the transfer of protein from nonspecific to cognate DNA. Since Eq. (4) applies for both cognate and nonspecific binding, this model provides a quantitative test for DNA-facilitated target search if the expected value of Δm_{tr} from Eq. (5) corresponds to the directly measured value from cognate binding in the presence of excess (100 μ M bp) nonspecific DNA. Fig. 4 shows the salt dependence of binding Elk1 to SC1 in the absence and presence of 100 μ M salmon sperm DNA, juxtaposed with existing data for ETV6 [9]. The presence of salmon sperm DNA induced a transition Na $^+$ concentration at 0.35 M Na $^+$ below which the apparent cognate affinity was reduced but the salt dependence was significantly flattened. Above 0.35 M Na $^+$, cognate binding was insensitive to the salmon sperm DNA as the nonspecific affinity was further weakened.

Using the salt-dependent data shown in Fig. 4, the calculated salt dependence for Blk1 transfer to SC1 is $\Delta m_{tr} = \Delta m_{sp} - \Delta m_{ns} = (-6.1 \pm$ $(0.1) - (-3.1 \pm 0.5) = -3.0 \pm 0.5$ according to Eq. (6). The observed value of Δm_{tr} in the presence of salmon sperm DNA at below 0.35 M Na⁺ is $\Delta m_{tr} = -2.9 \pm 0.2$ [Table 1]. The agreement between the expected and observed values of Δm_{tr} shows that under physiologically low-salt conditions (e.g., 0.15 M Na⁺), target recognition by long-range search is operative for Elk1 in the presence of 100 µM nonspecific DNA, even given its very high specificity. Remarkably, the transition Na⁺ concentration for Elk1 and ETV6 occurred at similar bulk salt concentrations of 0.35 M Na+, even though their respective cognate and nonspecific affinities were distinctly different. At 0.15 M Na+, the difference in apparent affinities between Elk1 and ETV6 in the presence of salmon sperm DNA is ~100-fold. Compared with the ~20-fold margin in the absence of nonspecific DNA, Elk1 is therefore even more selective relative to ETV6 when binding occurred by long-range target search.

To characterize the impact of selectivity on long-range target search more deeply, we examined Blk1 binding with its more preferred cognate sequence: the native E74 site found in Drosophila [18]. Measurement of E74 binding by Elk1 in the absence of nonspecific DNA showed ~3-fold higher affinity relative to SC1 [Fig. S3A, Supporting Information]. In the presence of salmon sperm DNA, the transition Na⁺ concentration was also similar at ~0.35 M Na+ with a similarly flattened salt dependence below that Na+ concentration [Fig. S3B]. As with SC1, the expected transfer ion number $\Delta m_{tr} = \Delta m_{sp} - \Delta m_{ns} = (-6.0 \pm 0.1) - (-3.1 \pm 0.5) = -2.9 \pm 0.5$ agrees with the measured value of -2.6 ± 0.8 below the transition [Na⁺] in the presence of salmon sperm DNA [Table 2]. The apparent KD was higher by ~3-fold relative to SC1 in the presence of salmon sperm DNA, a margin equal to the difference in intrinsic affinities between the two cognate DNA sites. Thus, the salt-induced switch from direct to long-range target search was not sensitive to the intrinsic affinities of the ligand to cognate DNA. The remaining parameter, the abundance of nonspecific

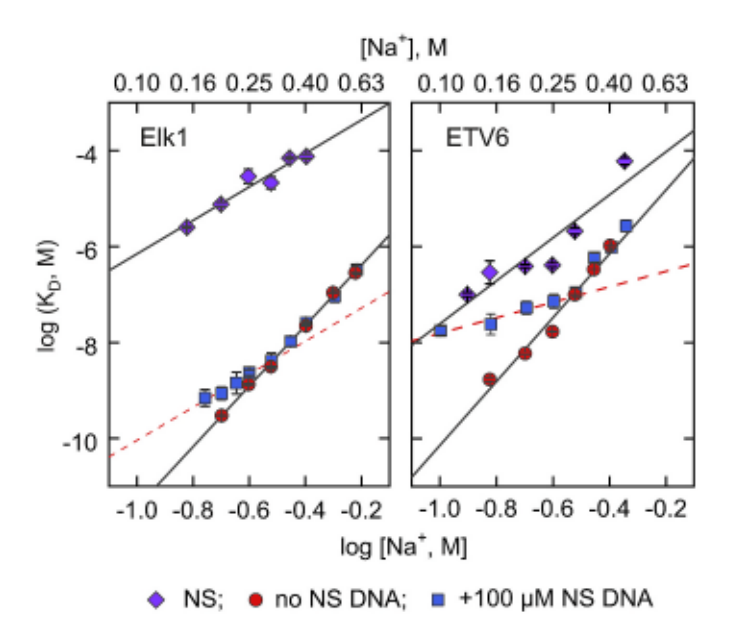


Fig. 4. Impact of DNA sequence selectivity on long-range target search ETS structural homologs: Elk1 vs ETV6. Comparison of salt dependence of equilibrium dissociation constants of Elk1 and ETV6 to SC1: cognate binding with (blue squares) and without (red circles) 100 μ M bp salmon sperm DNA, together with nonspecific binding (purple diamonds). The red dash line represents the best fit in the transfer régime in the presence of salmon sperm DNA in both panels. Numerical data for Elk1/SC1 binding under both conditions are given in Tables S1 and S2. Nonspecific binding for Elk1 is taken from Fig. S2. ETV6 data is from Ref. [9]. The salt dependence for nonspecific binding is $\Delta m_{ns} = -3.1 \pm 0.5$ for Elk1 and $\Delta m_{ns} = -4.5 \pm 0.9$ for ETV6. (For interpretation of the references to color in this figure legend, the reader is referred to the Web version of this article.)

Table 1 Salt-dependent Elk1/SC1 interactions.

Experimental conditions	$\Delta m = -alope$	2	K _D (nM) at 0.15 M Na ^{+a}
no NS DNA	-6.1 ± 0.1	7	0.06 ± 0.01
$+100 \mu M$ NS DNA $< 0.35 M$ Na	-2.9 ± 0.2	3	0.37 ± 0.08

Extrapolated.

DNA, thus appeared to be the governing factor.

Kinetic measurements of Elk1/DNA target search by biosensor-SPR. To probe the nature of long-range transfer more mechanistically, we examined the kinetics of cognate association and dissociation in the presence and absence of salmon sperm DNA. By maintaining Elk1 in a nonspecific complex prior to cognate binding at low salt, we were able to observe the time-dependent translocation of Elk1 onto cognate DNA. In the absence of salmon sperm DNA, the useable range of salt concentration for kinetic analysis is from 0.3 to 0.6 M Na+ [Fig. 5A]. Within the range, the kinetics of the specific interaction were within the temporal resolution of the instrument. The association and dissociation rate constants yielded a linear log-log relationship with salt concentration in this range. In the presence of salmon sperm DNA at 100 µM bp, the accessible salt range for kinetic analysis broadened from 0.175 to 0.6 M Na+. As Fig. 5A illustrates, the kinetics were well described by a 1:1 interaction. The millisecond time resolution of SPR instrumentation means that the apparent rate constants represent the rate-limit step of more rapid microscopic events. Armed with kinetic data over a range of salt conditions, the salt dependencies of the observed rate constants $(\Delta m_a$ and $\Delta m_d)$ are related to that for the equilibrium constant as

$$\Delta m_{\text{obs}} = -\frac{d \log K_{\text{D}}}{d \log[\text{Na}^+]} = \frac{d(\log k_{\text{a}} - \log k_{\text{d}})}{d \log[\text{Na}^+]} = \Delta m_{\text{a}} - \Delta m_{\text{d}}$$
 (7)

In the absence of salmon sperm DNA, the salt dependence obtained from association and dissociation rate constants for E74 binding by Elk1 is $\Delta m_a - \Delta m_d = (-5.1 \pm 0.1) - (1.3 \pm 0.1) = -6.4 \pm 0.1$ [Table 3]. This value was in agreement with that obtained from the steady-state equilibrium measurement under the same conditions ($\Delta m_{sp} = -6.0 \pm 0.1$). The goodness of fit for the kinetic data and agreement in salt dependence with equilibrium data supported interpretation of kinetics as a 1:1 interaction. In the presence of salmon sperm DNA, the kinetic profile showed two distinct régimes that transition sharply at 0.35 M Na⁺ [Fig. 5B], in step with the thermodynamic salt profile in Fig. 4. Above 0.35 M Na⁺, Elk1/E74 association was decelerated by increasing salt, a behavior expected of target search by free diffusion (e.g., charge screening by mobile ions in the flow solution), indicating that the protein has overcome trapping by nonspecific DNA in the flow solution. At Na+ concentrations below 0.35 M, association was accelerated by increasing bulk salt concentration, pointing to dissociation of nonspecific complexes as the rate-limiting step.

For comparison, we also characterized the kinetics of Elk1 with the lower-affinity cognate site, SC1. We observed similar agreement between the calculated value Δm_a - Δm_d [Table 4] and measured Δm_{sp} for E74 binding in the absence of salmon sperm DNA (Fig. S3B). The higher intrinsic affinity of Elk1 for E74 could be readily seen as due to faster association relative to SC1 at corresponding salt concentrations, while dissociation was little unchanged (Fig. 5B). Beyond the absolute values of the rate constants, their salt dependence reveals the ionic properties

Table 2 Salt-dependent Elk1/E74 interactions.

Experimental conditions	Δm = -alope	 s	K _D (nM) at 0.15 M Na ⁺⁸
no NS DNA	-6.0 ± 0.1	7	0.02 ± 0.01
+100 μM NS DNA, < 0.35 M Na ⁺	-2.6 ± 0.8	3	0.11 ± 0.05

^{*} Extrapolated.

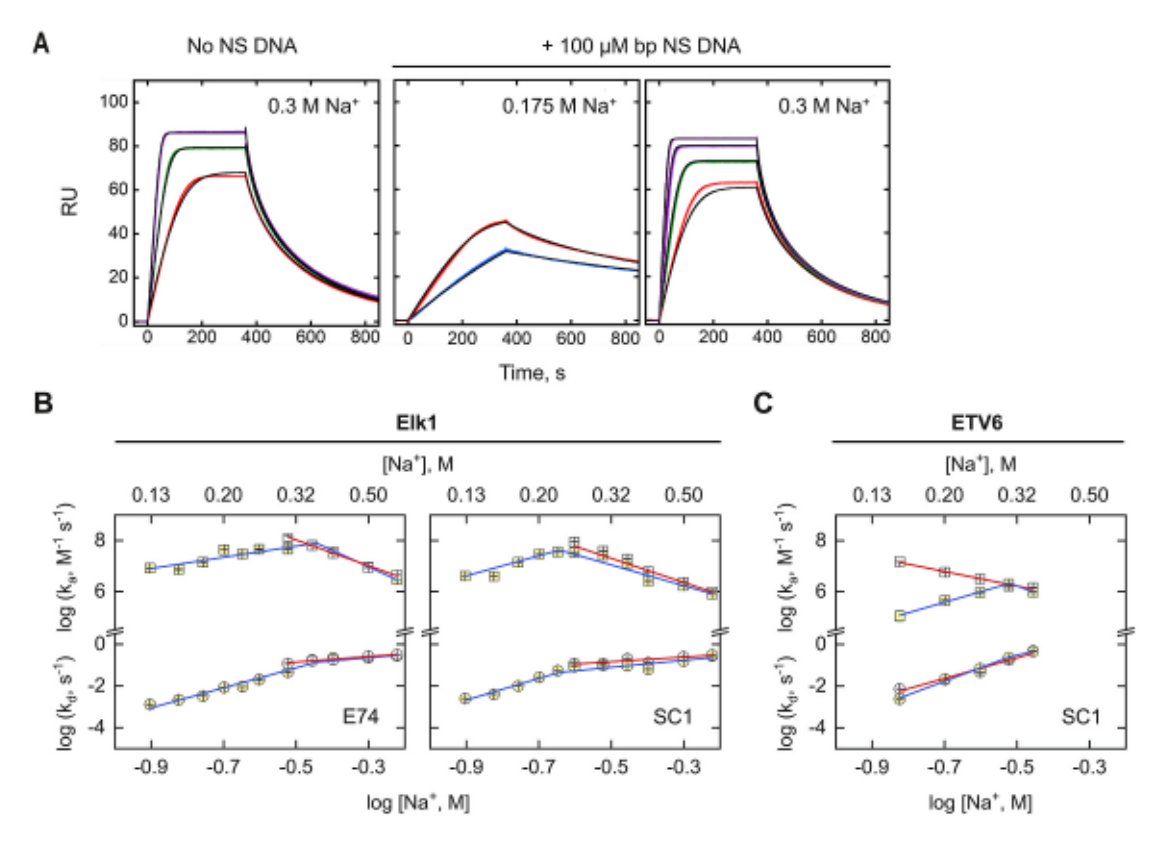


Fig. 5. Kinetic analysis of Elk1 interactions with cognate DNA in the absence and presence of excess nonspecific DNA. A, Representative sensorgrams (colored curves) with kinetic fit (black solid lines) for a 1:1 interaction of Elk1 under the indicated conditions. B and C, Salt dependence of apparent association (square) and dissociation rate constants (circles) in the absence (red line, uncolored symbols) and presence of 100 μM bp salmon sperm DNA (blue line, yellow symbols) for Elk1 binding E74 and SC1, as well as a previously reported ETV6/SC1 interaction [9]. Numerical data for Elk1 is given in Tables S1-S4. (For interpretation of the references to color in this figure legend, the reader is referred to the Web version of this article.)

of the activated complex along the binding interaction coordinate [3], 32]. The salt dependence in the association rate constant was more negative for E74 than SC] without salmon sperm DNA, and less positive in its presence. As Δm_{tr} in Eq. (6) provides information about the change in number of ionic contacts between the states at equilibrium, Δm_a and Δm_d provide analogous information about the activated complex [32]. The magnitudes of the differences in the salt dependence suggests that E74 binding from free solution required up to one more ionic contact in the activated complex that is not made with SC].

In the presence of salmon sperm DNA, absolute association rate constants were lower than the extrapolated values in the absence of salmon sperm DNA, indicating that long-range transfer was a net negative contribution to target search. Since the salmon sperm DNA was much longer than the immobilized target (>5 kbp vs. 23 bp), additional contributions from sliding and hopping on nonspecific DNA were included in the observed kinetics in the transfer régime. These myriad short- and long-range translocations along and between the nonspecific DNA polymers dynamically sequester the protein from populating the free state at equilibrium.

As a window into the mechanism of target search, dissociation kinetics are particularly useful for inferring the role of DNA-facilitated transfer in target search: if complex dissociation is unimolecular, it should not depend kinetically on another species in the solution. With

Table 3 Salt-dependent kinetics of Elk1/E74 binding.

Experimental conditions	Slope $k_a = \Delta m_a$	Slope $k_d = \Delta m_d$
no NS DNA	-5.1 ± 0.1	1.3 ± 0.1
+100 µM NS DNA < 0.35 M Na+	2.2 ± 0.4	4.8 ± 0.3
+100 µM NS DNA > 0.35 M Na+	-6.5 ± 0.7	1.5 ± 0.7

respect to ETV6 [9], kinetic measurements above ~0.5 M Na+ were severely limited by prohibitively fast dissociation kinetics [Fig. 5C]. In contrast, Blk1 enabled measurements of long-range target search, particularly dissociation kinetics, into significantly higher Na+ concentrations. The extended definition of dissociation kinetics, particularly in the case of the Elk1/SC1 interaction (Fig. 5B), provided new insight into the mechanism of long-range search. Below the transition Na⁺ at 0.35 M, the dissociation rate was markedly more salt dependent than in the absence of nonspecific DNA (Tables 3 and 4). This was expected based on the engagement of the transfer régime at equilibrium (Fig. 4). Above the transition salt concentration, the equilibrium constants were no longer sensitive to nonspecific DNA. If nonspecific DNA played no role under these conditions, one would expect the dissociation rate constants to be identical in the absence of nonspecific DNA. However, we observed that dissociation kinetics of Elk1 from SC1 remained salt-dependent in the presence of salmon sperm DNA (Table 4). This difference in salt dependence could not be ascribed to a passive alteration to the solution ionic strength by the DNA, which was dominated in concentration by NaCl. Additionally, the solution viscosity is not significantly altered by polymeric DNA at the concentration used [33]. In the case of E74, the precision of the rate constants above 0.35 M Na⁺ was not sufficient to differentiate from those measured without nonspecific DNA. This was due in part to the shorter span of Na+ concentrations over which

Table 4
Salt-dependent kinetics of Elk1/SC1 binding.

Experimental conditions	Slope $k_a = \Delta m_a$	Slope $k_{\mathrm{d}} = \Delta m_{\mathrm{d}}$
no NS DNA +100 µM NS DNA <0.35 M Na ⁺	-4.7 ± 0.1 3.9 ± 0.4	1.1 ± 0.2 5.2 ± 0.8
+100 μM NS DNA >0.35 M Na ⁺	-4.1 ± 0.3	1.7 ± 0.2

dissociation kinetics could be measured (Fig. 5B). The more salt-dependent dissociation kinetics in the presence of nonspecific DNA are consistent with additional ionic contacts made by the translocating activated complex that were not present in binding from free solution.

In summary, SPR-detected kinetics demonstrate that the protein is indeed interacting with both immobilized and nonspecific DNA as it transitions from one to the other. DNA-facilitated dissociation such as reported by Fried and Crothers [34] and further elaborated by the Marko and Johnson groups [6,35,36] is classically associated with homo- or hetero-multimeric DNA-binding proteins which transfer from one duplex to another via a multivalent, monkey bar mechanism [10 13]. In contrast, Elk1 and ETV6 form strictly 1:1 protein/DNA complexes. Dimeric binding by Elk1 and ETV6, such as found in some genomic contexts (Fig. 3C), require two copies of the ETS consensus sequences in close proximity. How do proteins with only one DNA-contact interface (i.e., no spare arms) achieve intersegmental translocation? One plausible mechanism is suggested by the fly-casting model of DNA association that has been postulated in computational work by Wolynes and coworkers [37]. In the fly-casting model, the electrostatic field of nearby DNA induces transient unfolding of the protein which refolds upon formation of the specific complex [37]. Since the formation of protein/DNA complexes proceeds through ionically distinct activation complexes, differences in the observed salt-dependent kinetics due to presence of nonspecific DNA are consistent with a fly-casting-type transient intermediate. We therefore postulate that the protein undergoes a conformational change to form a transient ternary complex with both cognate and nonspecific DNA. Based on the dissociation kinetics for the Elk1/SC1 complex, this transient complex contains, at the rate-limiting step, one more ionic contact with cognate and nonspecific DNA than the equilibrium cognate complex (c.f. Fig. 3A).

4. Conclusion

Comparison of Elk1 binding to cognate sites of different affinities as well as with its structural homolog ETV6 has significantly extended the use of biosensor-SPR in gaining insight into long-range target search by DNA-binding proteins. The new measurements indicate that long-range target search across disconnected DNA strands is robust to even a high intrinsic selectivity ratio. As the comparison between Elk1 and ETV6 shows, engagement of long-range transfer reinforces relative selectivity even as the effect on apparent affinity is negative. Comparison of the dissociation kinetics reveals evidence of transient ionic interactions that indicate DNA-facilitated dissociation for proteins with only single DNAbinding surfaces. This evidence generalizes DNA-to-DNA transfer as a long-range search mechanism beyond the subset of proteins with multiple DNA-binding interfaces. We therefore revise our original model for proteins with single DNA-binding sites [9] in that a transiently unbound species during translocation no longer appears necessary. Instead, a transient ternary intermediate in which the protein is contacting both nonspecific and cognate DNA is discernible at the rate-limiting step. For ETS proteins and other examples that fold stably at equilibrium, significant transient dynamics of the folded conformation are implied, even if their exact nature remains currently elusive.

Methodologically, our work adds DNA target search to a growing field of novel biosensor applications and immediately suggests new avenues of investigations (e.g., impact of competing ligands on DNA target search). Compared with other real-time bioanalytical techniques, biosensor-SPR is relatively generous in terms of sample requirements and ease of deployment, and therefore offers significant merit to the community.

Funding

This work was supported by the National Science Foundation [grant number MCB 2028902] and the National Institutes of Health [grant numbers GM111749 and HL155178]. T.V. was supported by a GSU Molecular Basis of Disease Fellowship.

Author contributions

W.D.W. and T.V. designed the experiments, which were performed by T.V. G.M.K.P. prepared the recombinant Elk1 protein. T.V., A.L.S., W. D.W. and G.M.K.P. analyzed the data. All authors contributed to the conception and design of this work as well as preparation of the manuscript. The authors acknowledge with thanks suggestions provided by the reviewers.

Declaration of interest

There are no conflicts of interest to declare.

Appendix A. Supplementary data

Supplementary data to this article can be found online at https://doi. org/10.1016/j.ab.2021.114298.

References

- N.P. Stanford, M.D. Szczelkun, J.F. Marko, S.E. Halford, One- and threedimensional pathways for proteins to reach specific DNA sites, EMBO J. 19 (2000) 6546–6557.
- [2] S.E. Halford, J.F. Marko, How do site-specific DNA-binding proteins find their targets? Nucleic Acids Res. 32 (2004) 3040–3052.
- [3] Q. Szabo, F. Bantignies, G. Cavalli, Principles of genome folding into topologically associating domains, Sci Adv 5 (2019), eaaw1668.
- [4] N. Sikorska, T. Sexton, Defining functionally relevant spatial chromatin domains: it is a TAD complicated, J. Mol. Biol. 432 (2020) 653 664.
- [5] H. Willenbrock, D.W. Ussery, Chromatin architecture and gene expression in Escherichia coli, Genome Biol. 5 (2004) 252.
- [6] R.D. Giuntoli, N.B. Linzer, E.J. Banigan, C.E. Sing, M.O. de la Cruz, J.S. Graham, R. C. Johnson, J.F. Marko, DNA-Segment-Facilitated dissociation of fis and NHP6A from DNA detected via single-molecule mechanical response, J. Mol. Biol. 427 (2015) 3123–3136.
- [7] N. Shimamoto, One-dimensional diffusion of proteins along DNA. Its biological and chemical significance revealed by single-molecule measurements, J. Biol. Chem. 274 (1999) 15293 15296.
- [8] L. Finzi, J. Gelles, Measurement of lactose repressor-mediated loop formation and breakdown in single DNA molecules, Science 267 (1995) 378–380.
- [9] T. Vo, S. Wang, G.M.K. Poon, W.D. Wilson, Electrostatic control of DNA intersegmental translocation by the ETS transcription factor ETV6, J. Biol. Chem. 292 (2017) 13187 13196.
- [10] J. Rudolph, J. Mahadevan, P. Dyer, K. Luger, Poly(ADP-ribose) polymerase 1 searches DNA via a monkey bar mechanism, Elife 7 (2018).
- [11] T.Y. Chen, Y.S. Cheng, P.S. Huang, P. Chen, Facilitated unbinding via multivalency-enabled ternary complexes: new paradigm for protein-DNA interactions, Acc. Chem. Res. 51 (2018) 860–868.
- [12] B.A. Lieberman, S.K. Nordeen, DNA intersegment transfer, how steroid receptors search for a target site, J. Biol. Chem. 272 (1997) 1061 1068.
- [13] A.J. Pollak, A.T. Chin, F.L.H. Brown, N.O. Reich, DNA looping provides for intersegmental hopping by proteins: a mechanism for long-range site localization, J. Mol. Biol. 426 (2014) 3539 3552.
- [14] A.V. Albrecht, H.M. Kim, G.M.K. Poon, Mapping interfacial hydration in ETS-family transcription factor complexes with DNA: a chimeric approach, Nucleic Acids Res. 46 (2018) 10577 10588.
- [15] D.C. Stephens, G.M. Poon, Differential sensitivity to methylated DNA by ETS-family transcription factors is intrinsically encoded in their DNA-binding domains, Nucleic Acids Res. 44 (2016) 8671–8681.
- [16] S. Wang, M.H. Linde, M. Munde, V.D. Carvalho, W.D. Wilson, G.M. Poon, Mechanistic heterogeneity in site recognition by the structurally homologous DNAbinding domains of the ETS family transcription factors Ets-1 and PU.1, J. Biol. Chem. 289 (2014) 21605–21616.
- [17] S. Xhani, S. Esaki, K. Huang, N. Erlitzki, G.M. Poon, Distinct roles for interfacial hydration in site-specific DNA recognition by ETS-family transcription factors, J. Phys. Chem. B 121 (2017) 2748 2758.
- [18] P. Shore, L. Bisset, J. Lakey, J.P. Waltho, R. Virden, A.D. Sharrocks, Characterization of the elk-1 ETS DNA-binding domain, J. Biol. Chem. 270 (1995) 5805–5811.
- [19] D.C. Stephens, H.M. Kim, A. Kumar, A.A. Farahat, D.W. Boykin, G.M.K. Poon, Pharmacologic efficacy of PU.1 inhibition by heterocyclic dications: a mechanistic analysis, Nucleic Acids Res. 44 (2016) 4005–4013.
- [20] M. Munde, G.M. Poon, W.D. Wilson, Probing the electrostatics and pharmacological modulation of sequence-specific binding by the DNA-binding domain of the ETS family transcription factor PU.1: a binding affinity and kinetics investigation, J. Mol. Biol. 425 (2013) 1655 1669.
- [21] S. Wang, G.M.K. Poon, W.D. Wilson, Quantitative investigation of protein nucleic acid interactions by biosensor surface plasmon resonance, in: B.P. Leblanc, S. Rodrigue (Eds.), DNA-protein Interactions, Springer, New York, 2015, pp. 313–332.

- [22] F.A. Tanious, W. Laine, P. Peixoto, C. Bailly, K.D. Goodwin, M.A. Lewis, E.C. Long, M.M. Georgiadis, R.R. Tidwell, W.D. Wilson, Unusually strong binding to the DNA minor groove by a highly twisted benzimidazole Diphenylether: induced fit and bound water, Biochemistry 46 (2007) 6944–6956.
- [23] M.T. Weirauch, A. Yang, M. Albu, A.G. Cote, A. Montenegro-Montero, P. Drewe, H. S. Najafabadi, S.A. Lambert, I. Mann, K. Cook, H. Zheng, A. Goity, H. van Bakel, J. C. Lozano, M. Galli, M.G. Lewsey, E. Huang, T. Mukherjee, X. Chen, J.S. Reece-Hoyes, S. Govindarajan, G. Shaulsky, A.J.M. Walhout, F.Y. Bouget, G. Ratsch, L. F. Larrondo, J.R. Ecker, T.R. Hughes, Determination and inference of eukaryotic transcription factor sequence specificity, Cell 158 (2014) 1431 1443.
- [24] C.T. Workman, Y. Yin, D.L. Corcoran, T. Ideker, G.D. Stormo, P.V. Benos, enoLOGOS: a versatile web tool for energy normalized sequence logos, Nucleic Acids Res. 33 (2005) W389 W392.
- [25] M.T. Record Jr., C.F. Anderson, T.M. Lohman, Thermodynamic analysis of ion effects on the binding and conformational equilibria of proteins and nucleic acids: the roles of ion association or release, screening, and ion effects on water activity, Q. Rev. Biophys. 11 (1978) 103 178.
- [26] M.T. Record, T.M. Lohman, A semiempirical extension of polyelectrolyte theory to the treatment of oligoelectrolytes: application to oligonucleotide helix-coil transitions, Biopolymers 17 (1978) 159 166.
- [27] Y. Mo, B. Vaessen, K. Johnston, R. Marmorstein, Structure of the elk-1-DNA complex reveals how DNA-distal residues affect ETS domain recognition of DNA, Nat. Struct. Biol. 7 (2000) 292 297.
- [28] T.D. Vo, A.L. Schneider, W.D. Wilson, G.M.K. Poon, Salt bridge dynamics in protein/DNA recognition: a comparative analysis of Elk1 and ETV6, Phys. Chem. Chem. Phys. 23 (2021) 13490 13502.

- [29] J.D. McGhee, P.H. von Hippel, Theoretical aspects of DNA-protein interactions: cooperative and non-co-operative binding of large ligands to a one-dimensional homogeneous lattice, J. Mol. Biol. 86 (1974) 469 489.
- [30] A. Jolma, J. Yan, T. Whitington, J. Toivonen, K.R. Nitta, P. Rastas, E. Morgunova, M. Enge, M. Taipale, G. Wei, K. Palin, J.M. Vaquerizas, R. Vincentelli, N. M. Luscombe, T.R. Hughes, P. Lemaire, E. Ukkonen, T. Kivioja, J. Taipale, DNA-binding specificities of human transcription factors, Cell 152 (2013) 327–339.
- [31] T.M. Lohman, Kinetics of protein-nucleic acid interactions: use of salt effects to probe mechanisms of interaction, CRC Crit. Rev. Biochem. 19 (1986) 191–245.
- [32] T.M. Lohman, P.L. DeHaseth, M.T. Record Jr., Analysis of ion concentration effects of the kinetics of protein-nucleic acid interactions. Application to lac repressoroperator interactions, Biophys. Chem. 8 (1978) 281 294.
- [33] E.L. Gilroy, M.R. Hicks, D.J. Smith, A. Rodger, Viscosity of aqueous DNA solutions determined using dynamic light scattering, Analyst 136 (2011) 4159 4163.
- [34] M.G. Fried, D.M. Crothers, Kinetics and mechanism in the reaction of gene regulatory proteins with DNA, J. Mol. Biol. 172 (1984) 263 282.
- [35] R.I. Kamar, E.J. Banigan, A. Erbas, R.D. Giuntoli, M. Olvera de la Cruz, R. C. Johnson, J.F. Marko, Facilitated dissociation of transcription factors from single DNA binding sites, Proc. Natl. Acad. Sci. U. S. A. 114 (2017) E3251 E3257.
- [36] A. Erbas, J.F. Marko, How do DNA-bound proteins leave their binding sites? The role of facilitated dissociation, Curr. Opin. Chem. Biol. 53 (2019) 118 124.
- [37] Y. Levy, J.N. Onuchic, P.G. Wolynes, Fly-casting in protein-DNA binding: frustration between protein folding and electrostatics facilitates target recognition, J. Am. Chem. Soc. 129 (2007) 738 739.